Z Dependence of Positive Photopion Production*

W. S. C. WILLIAMS,† K. M. CROWE,‡ AND R. M. FRIEDMAN§
Department of Physics and High-Energy Physics Laboratory, Stanford University, Stanford, California

(Received December 10, 1956)

The Z dependence of positive photopion production has been measured with 550-Mev bremsstrahlung. The data are compared with the optical model using the real and imaginary potentials given by Frank, Gammel, and Watson. If variations in the production cross section due to the real potential, including the Coulomb potential, are taken into account, the agreement for pion energies in the range 33 to 152 Mev is surprisingly good considering both the approximations in the model and the experimental errors. The observed absorption mean free path varies from $\sim 9\times 10^{-13}$ cm for 33-Mev pions to $\sim 1\times 10^{-13}$ cm at the highest energies.

I. INTRODUCTION

THE Z dependence of positive pions produced by 350-Mev bremsstrahlung has been studied by Mozley (π^+),[1] Littauer and Walker (π^+ and π^-),[2] and more recently by Imhof, Perez-Mendez, and Easterday (π^+).[3] Neutral photomesons have been measured by Panofsky *et al.*,[4] and Anderson *et al.*[5]; and Hales[6] has studied both photoproduced and proton-produced π^0's. The Z dependence of pion production by protons has also been studied by a number of experimenters.[7–9] The results are usually interpreted as indicating that the reduction of pion production per nucleon in the heavy elements can be accounted for by absorption of mesons produced in the interior of the nucleus. In the first approximation the yield will follow an $A^{\frac{2}{3}}$ dependence for nuclei whose radii are large compared to the mean free path of mesons in nuclear matter.[10] Some deviations from this rule have been observed and the explanation may be extremely complicated; the Coulomb barrier corrections,[11] the details of nuclear final states, variations in nucleon momentum distributions, etc., are certainly involved.

In 1952, results from the California Institute of Technology[12] indicated a resonance in pion photoproduction from hydrogen. Our work was begun to see if there is any similar resonance behavior in complex nuclei. Recently, improvement in the counting apparatus has allowed us to improve the results considerably, and only the later results are reported here.

II. EXPERIMENTAL EQUIPMENT

The details of our pion-counting apparatus are given elsewhere.[13] In this study, a bremsstrahlung beam was produced by running the 550-Mev electron beam of the Stanford Mark III linear accelerator[14] through an 0.010-in. tantalum radiator. The electron beam current was integrated with a secondary-emission monitor[15] and subsequently bent out of the photon beam with a small deflecting magnet. The position of the photon beam was observed with a CsBr crystal visually, and was seen to be ~ 1 in. in diameter. Pion production was studied at an angle of 60° in the laboratory. Targets were placed bisecting the angle between the beam and the pion channel. The targets were made small to reduce corrections due to photon absorption and the pion energy loss. The characteristics of the targets used are given in Table I.

Pions were selected by momentum with a crude analyzing magnet with large aperture and relatively poor resolution ($\Delta P/P \simeq 15\%$ full width at half-maximum). The positive pions stopped in a large plastic scintillator and decayed into muons. Only the delayed

* The research reported here was supported by the joint program of the Office of Naval Research and the U. S. Atomic Energy Commission.

† Now with the Department of Natural Philosophy, The University, Glasgow, Scotland.

‡ Now with the University of California Radiation Laboratory, Berkeley, California.

§ Now with Lockheed Aircraft Corporation, Missile Systems Division, Palo Alto, California.

1 R. F. Mozley, Phys. Rev. **80**, 493 (1950).

2 R. M. Littauer and D. Walker, Phys. Rev. **86**, 838 (1952).

3 W. L. Imhof, University of California Radiation Laboratory Report UCRL-3383 (unpublished); Imhof, Perez-Mendez, and Easterday, Phys. Rev. **100**, 1798(A) (1955).

4 Panofsky, Steinberger, and Steller, Phys. Rev. **86**, 180 (1952).

5 Anderson, Kenny, and McDonald, Phys. Rev. **100**, 1798 (1955); J. D. Anderson, University of California Radiation Laboratory Report UCRL-3426 (unpublished).

6 R. W. Hales, University of California Radiation Laboratory Report UCRL-1836 (unpublished).

7 D. L. Clark, Phys. Rev. **87**, 157 (1952).

8 J. Merritt and D. A. Hamlin, Phys. Rev. **99**, 1523 (1955); J. Merritt, University of California Radiation Laboratory Report UCRL-2424 (unpublished).

9 R. Sagane and W. F. Dudziak, Phys. Rev. **92**, 212 (1953); W. F. Dudziak and R. Sagane, University of California Radiation Laboratory Report UCRL-2304 (unpublished); W. F. Dudziak, University of California Radiation Laboratory Report UCRL-2564 (unpublished).

10 The $A^{\frac{2}{3}}$ dependence usually mentioned comes from assuming equal production from A nucleons times an absorption factor proportional to λ_{abs}/R, where $R=R_0A^{\frac{1}{3}}$. Assuming equal production from protons only, this $A^{\frac{2}{3}}$ dependence should be multiplied by the proton-nucleon ratio (Z/A), giving a final behavior of $ZA^{-\frac{1}{3}}$. To smooth out the variations in the π^-/π^+ ratios near threshold, Littauer and Walker (reference 2) chose to combine π^+ with π^- yields. At our energies, there are no significant π^-/π^+ ratio variations, so that our results would be unchanged by combining the π^- and π^+ cross sections.

11 S. Gasiorowicz, Phys. Rev. **93**, 843 (1954).

12 Walker, Teasdale, Peterson, and Vette, Phys. Rev. **99**, 210 (1955); Tollestrup, Keck, and Worlock, Phys. Rev. **99**, 220 (1955).

13 Motz, Crowe, and Friedman (to be published).

14 M. Chodorow *et al.*, Rev. Sci. Instr. **26**, 134 (1955); W. K. H. Panofsky and J. A. McIntyre, Rev. Sci. Instr. **25**, 287 (1954).

15 G. W. Tautfest and H. R. Fechter, Rev. Sci. Instr. **26**, 229 (1955).

positrons were counted after the 0.1-μsec beam pulse was finished. Various time channels up to 20 μsec and two pulse-height discriminator channels were recorded.

The backgrounds in this experiment were of four types: (1) Pions produced in the air: ~10–20% of the signal due to our choice of small targets; (2) Probable delayed neutron activities with a long half-life, most of which came from the radiator and other objects in the electron beam, including the area in which the beam is absorbed; (3) The long period neutron background from the targets: measured to be $\leq 5\%$ in the worst case; (4) Possible charged particles other than pions that might deflect in the field. Background (1) was measured by removing the target at each energy setting, (2) by turning the magnet off with no target in place, and (3) with the field off and subtracting the no-target from the target yields. Background (4) was probably due to either muons or β particles since protons would not satisfy the requirements of range, momentum, and pulse height set by the detection system. There was no significant long-period signal coming from the target and deflected with the magnet. Muons from pion decays in flight were counted and their effect on the π^+ energy resolution is negligible.[16] The only known source of background β-particles with the proper decay period is from μ-β decay in the target, coming from muons produced by low-energy pions that stopped in the target. These events were observed for appropriately small fields (positive particles) in the deflecting magnet; this signal cut off well below the lowest setting used.

The net target yields were obtained by subtracting the backgrounds measured under various conditions. Some of the small background corrections that are not measurable were obtained as upper limits in the worst cases and scaled to the more favorable ones.

The pion energies were varied as follows: $T_\pi = 91$, 123, 152, 185 Mev were obtained by setting the magnet at 64 Mev and adding appropriate absorbers as close as possible to the target ahead of the collimating channel; $T_\pi = 33$, 64, 91 Mev were obtained with different magnet settings. The 91-Mev results obtained by both methods agree within the errors. The spectrum of pions from carbon was measured; we are not directly concerned here with either measurements of carbon absolute cross sections or carbon excitations, and the results of these measurements are reported elsewhere.[17]

TABLE I. Target characteristics.

Material	Thickness g/cm²	Radiation length	Average pion energy loss (ΔE) $T_\pi = 33$ Mev	$T_\pi = 185$ Mev
Li	1.362	0.058	3.65	1.42
C	0.856	0.020	2.00	0.96
Al	0.840	0.035	1.75	0.84
Cu	0.955	0.075	1.65	0.83
Ta	0.843	0.132	1.22	0.61
U	0.777	0.145	1.03	0.52

III. ERRORS

The results will be quoted with their statistical errors. The main source of systematic error is, we believe, the variations in over-all gain which cause the counting efficiency to vary. There are both short- and long-period variations in efficiency: the long-time variation arising from temperature variation or component fatigue can be eliminated by cycling any measurement several times rapidly enough to cancel out the drift; the effects of short-time fluctuations are also minimized by keeping the net weight of a single run small. Data were obtained from a combination of several separate cycles, and the reproducibility was used to decide if any obvious instability was present. In practice, it was not possible for us to detect definitely any small efficiency variations of, for example, less than 10%, with the present electronic instrumentation. By analyzing the internal and external errors of a number of runs, we believe that the estimate of the standard deviation derived from statistics alone is probably not in error by more than 50%, and certainly a factor of two would be extremely pessimistic.

IV. RESULTS

The results for five pion energies are shown in Figs. 1–5. We have plotted the yield divided by $A^{\frac{2}{3}}$ on a logarithmic scale *vs* *Z*. The presentation allows the theoretical curves to be shifted vertically without altering their shape. The data have been normalized to the measured copper point (with the exception of

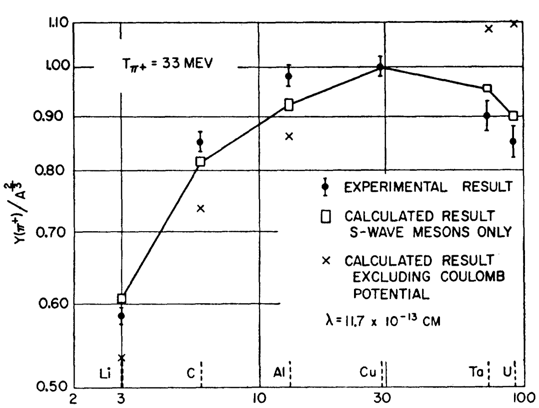

FIG. 1. The π^+ yield obtained from 550-Mev bremsstrahlung on targets of Li, C, Al, Cu, Ta, and U. The yield divided by $A^{\frac{2}{3}}$ is plotted for pions of 33 Mev. The curve shown using an absorption mean free path of 11.7×10^{-13} cm is normalized to the copper point. The crosses are the theoretical values neglecting the Coulomb effects. The nuclear radius was taken to be $1.4A^{\frac{1}{3}} \times 10^{-13}$ cm. Our choice for mean free path is $(9 \pm 2) \times 10^{-13}$ cm.

[16] This effect was largest at the lowest analyzing-magnet setting ($T_\pi = 33$ Mev). In this case, we estimate approximately 6% of the signal was from muons arising from the decay in flight of ~100-Mev pions. For higher energy settings, the effect was smaller. See reference 13 for a more detailed discussion.

[17] K. M. Crowe and R. M. Friedman (to be published).

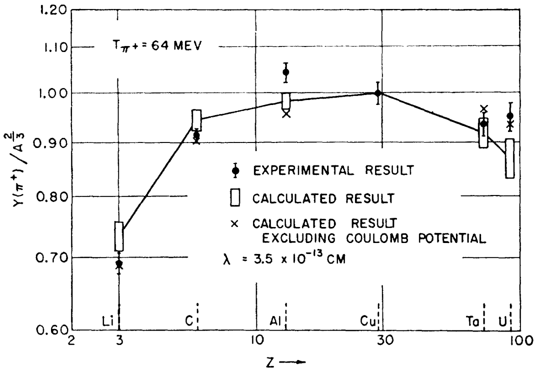

FIG. 2. The 64-Mev π^+ yields normalized to copper. The mean free path used in the calculation was taken to be 3.5×10^{-13} cm, and the estimated mean free path was $(4_{-1}^{+4})\times10^{-13}$ cm.

Fig. 3). The results show that there is considerable variation in this normalized yield relative to copper in the lithium and carbon measurements. Table II shows the observed cross sections obtained by normalizing these data to the carbon absolute cross-section measurements.[17]

We have calculated the relative π^+ yields with the optical model[18] using various mean free paths and assuming uniform production throughout the nucleus. For simplicity we have also assumed that the neutrons and protons uniformly occupy a sphere of radius $1.4A^{\frac{1}{3}}\times10^{-13}$ cm. The theoretical curves are also plotted in Figs. 1–5. For the low-energy pions the Coulomb potential due to the nuclear charge density must be taken into account. The nuclear charge has the following effects: (1) The distortion of the meson wave function by the Coulomb potential suppresses the positive-meson production. (2) The Coulomb potential energy for the pion in the nucleus alters the depth of the real potential, which in turn alters the cross section for the pion production. Calculations of these corrections (outlined in the Appendix) are complicated by our ignorance of the meson wave functions in nuclear matter; for example, the real and imaginary potentials for mesons in a nucleus are velocity-dependent, and have been estimated by Frank, Gammel, and Watson.[19] For the large nuclei the angular momentum meson states, other than s-states, must be considered even though the pions are of relatively low energy. An indication of the size of these effects is given for the worst case, $T_\pi=33$ Mev for uranium. For s-wave mesons, the barrier penetration factor relative to copper is 0.983 and the cross section is reduced by a factor 0.830. The theoretical curves in the figures indicate the yield corrected for absorption, with and without the Coulomb effect. The potentials and mean free paths used in the calculations are taken from Frank *et al.*,[19] and are shown in Table III.

The results for 33-Mev pion energy (Fig. 1) show that the Coulomb correction brings the data into fair agreement with a mean free path of 11.7×10^{-13} cm. The correction was calculated assuming only s-wave mesons. If a small amount of p-wave mesons is included or if the nuclear radius is reduced, the data and theory can be brought into coincidence. We estimate that the mean free path to get the best fit would be $(9\pm2)\times10^{-13}$ cm. The results for 64-Mev are shown in Fig. 2. The rectangles for the theory represent the uncertainty in the Coulomb corrections. The largest correction (measured from the uncorrected crosses) is an overestimate of the correction assuming all p-wave pions and a momentum-cubed variation in the production cross section. The other extreme of the band is that obtained assuming pure s-wave pion production. The agreement does not improve significantly by including the correction. The aluminum point is two standard deviations off and the deviation may represent a fluctuation in the detection efficiency discussed in the previous section. In Fig. 3

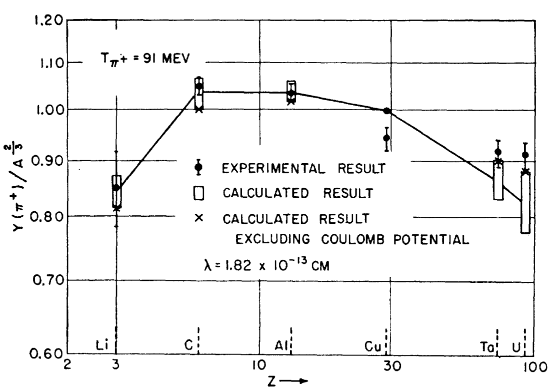

FIG. 3. The 91-Mev π^+ yields normalized to the aluminum point; the choice of normalization indicates that the copper point is probably in error. For the curves the mean free path was taken to be 1.82×10^{-13} cm. Our estimate from the data is $(1\pm0.5)\times10^{-13}$ cm.

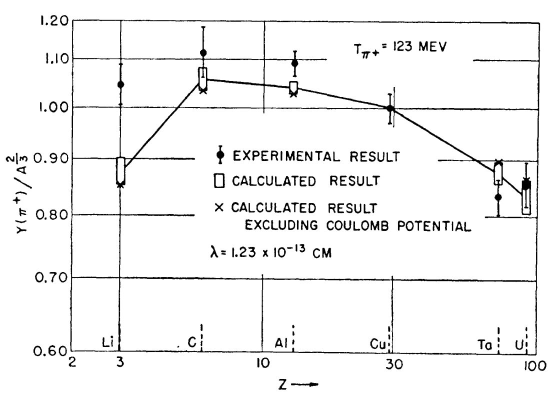

FIG. 4. The 123-Mev π^+ yields normalized to copper. The theoretical curve assumes $\lambda=1.27\times10^{-13}$ cm. Because the lithium point is high, we choose $(0.5_{-0.2}^{+0.3})\times10^{-13}$ cm for the best fit.

[18] Fernbach, Serber, and Taylor, Phys. Rev. **75**, 1352 (1949); Brueckner, Serber, and Watson, Phys. Rev. **84**, 258 (1951); K. M. Watson, Phys. Rev. **89**, 575 (1953); N. C. Francis and K. M. Watson, Phys. Rev. **89**, 328 (1953).

[19] Frank, Gammel, and Watson, Phys. Rev. **101**, 891 (1956).

TABLE II. Observed π^+ photoproduction cross sections for 550-Mev bremsstrahlung at a laboratory angle of 60°. The cross sections were obtained by normalizing the data of this experiment to the carbon measurements described in reference 17. Only the statistical errors of each measurement are shown. The normalization error is 8%. The values are quoted in units of 10^{-32} cm²/sterad-Mev-Q.

T_π (Mev)	H[a]	Li	C	Al	Cu	Ta	U
33	6.15±0.5	10.3 ±0.2	21.4±0.5	42.2±1.0	76.8±1.6	138 ±5	156 ±5
64	8.33±0.5	15.9 ±0.3	30.0±0.4	59.1±1.2	100 ±3	187 ±5	228 ±7
91	9.35±0.4	21.3 ±1.7	37.8±0.7	63.9±1.2	103 ±3	207 ±6	238 ±7
123	9.45±0.4	10.0 ±0.4	15.2±0.8	25.5±0.6	41.4±1.2	68.7±2.8	84.9±4.5
152	8.01±0.3	6.63±0.15	9.3±0.2	16.2±0.4	28.0±0.6	53.9±1.9	64.9±2.5
185	5.56±0.2	2.42±0.13	···	···	11.7±1.2	···	···

[a] The average hydrogen cross sections reported by Walker *et al.* (reference 12) have been included here for comparison.

the 91-Mev results are given. The normalization was shifted to the aluminum point since the fit indicates that the copper point was ~2–3 standard deviations away from the best fit. The 123-Mev results shown in Fig. 4 show an appreciable decrease from the $A^{2/3}$ law for the heavy elements U and Ta, in agreement with the very short mean free path and the surface proton-to-neutron ratio, which has already been included in the calculations.[10] The Li point being high indicated a shorter mean free path $\sim(0.5_{-0.2}^{+0.3})\times10^{-13}$ cm. It is not expected that the optical model will predict the yield for the small nuclei, especially when the mean free path is comparable with the nucleon spacing; therefore we do not attach any significance to this apparently very short mean free path. Figure 5 indicates the 152-Mev results. If one takes the discrepancy with the high-*Z* elements seriously, this indicates that the 152-Mev pions have already passed the resonance in the absorption mean free path.

In Table III the values for the absorption mean free paths, which we have picked to give a best fit,[20] are shown along with the estimated uncertainty of this measurement.

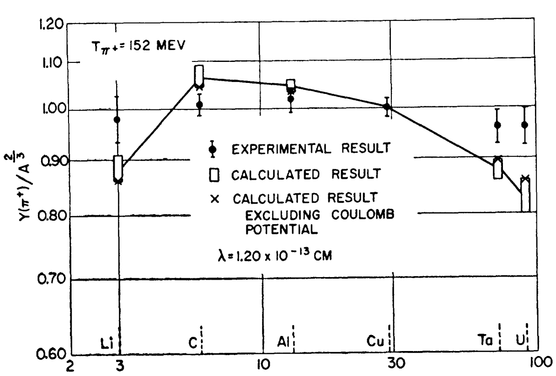

FIG. 5. The 152-Mev π^+ yields normalized to copper. The theoretical curve was made assuming 1.20×10^{-13} cm for the mean free path. Our estimate from the data is $\lambda=(2\pm1)\times10^{-13}$ cm.

[20] If the choice of mean free path is based on the heavy-element results alone [ignoring the results for elements lighter than copper and neglecting the Coulomb potential energy correction to the cross section (see Appendix)], the result is $\sim1\text{–}2\times10^{-13}$ cm. This type of analysis is used by Imhof *et al.* (reference 3). The data probably are not sufficiently accurate to show internal inconsistencies with their mean free path assignments.

The results clearly indicate a large variation of the mean free path in nuclear matter with pion energy. Since the fit in some cases is only fair, the errors assigned to the mean free paths are a combination of the statistical uncertainties in the data and a crude estimate of the quality of the fit.

V. DISCUSSION

A number of other points relate these data to work already done on the subject. (1) We suspect that by using lower-energy bremsstrahlung a number of effects can influence the *Z* dependence so as to obscure the absorption effect. For example, it has been observed[17] that for carbon the yield of pions per proton, as compared to hydrogen, varies from ~1/3 at 300 Mev to ~2/3 at 600 Mev. The sensitivity of this yield *vs* primary energy to the energetic threshold for pion production or to possible differences in momentum distribution in different elements can scarcely be ignored,[21] and it is not clear that even at 550 Mev we are justified in neglecting such effects.

(2) The neutron-proton ratio correction[10] is clearly sensitive to nucleon densities at the shell, which we have assumed is equal to the average neutron-proton ratio; this assumption is based on a study of the variation in neutron-proton ratio made by measuring the photoproduced π^-/π^+ ratio.[13] The results indicate

TABLE III. Parameters used in the calculation of the theoretical curves. T_π (lab) is the energy of the pion measured by the detection system; T_π (eff) is the pion kinetic energy in the nucleus ($Z=0$); V_R is the real potential and V_I the imaginary potential, taken from Frank *et al.* (reference 19); λ is the absorption mean free path; λ (est) is the mean free path obtained from the data with its uncertainties.

T_π (lab) (Mev)·····	33	64	91	123	152
T_π (eff) (Mev)······	53	106	134	156	169
V_R (Mev)··········	−20	−42	−43	−33	−17
V_I (Mev)··········	5.8	23	46	68	73
λ (10^{-13} cm)········	11.7	3.5	1.82	1.23	1.20
λ (exp) (10^{-13} cm)···	9±2	4_{-1}^{+4} [a]	1.5±0.5	$0.5_{-0.2}^{+0.3}$	2±1

[a] The high error is associated with the aluminum point; if this point is disregarded, the result is λ (est) $=(4\pm1)\times10^{-13}$ cm.

[21] Wattenberg, Odian, Stein, Wilson, and Weinstein, Phys. Rev. **104**, 1710 (1956). Their results indicate Li to have an internal momentum distribution corresponding to a Gaussian with a $1/e$ value of 8 Mev compared with carbon and oxygen of 18 and 19 Mev, respectively.

no deviations in the π^-/π^+ ratio from the average neutron-proton ratio to within 10%.[22]

(3) The effects of pion-pair production on the low-energy points must be considered.[23] For hydrogen the π^- and π^+ pair cross sections are less than 10–20% of the single-production cross section with 550-Mev bremsstrahlung, and we can probably assume the Z dependence of the pair processes will not be substantially different from that of the single-pion process.

(4) The mean free path derived from this work is about equal to that obtained from the total cross section for pions of the same kinetic energy in nuclear matter. The absorption clearly eliminates pions whereas for the scattering of a quasi-elastic character the situation is more complicated. A pion produced at a given energy scatters to a lower energy band. The pions that scatter inelastically lose sufficient energy to contribute to the lower energy pion bands only. Inelastic pions that scatter off of moving nucleons tend to lose a large fraction of their energy since pions up to 200 Mev prefer to scatter in the backwards direction.[24] In addition, the scattering of pions in the nuclear medium which degrades the pion energy results in a much larger change in energy measured outside the nucleus as a result of the rapid variation of the real potential.[25] The experimental results on the inelastic scattering of 100-Mev pions obtained by Bernardini *et al.*[26] show this behavior. The inelastic scattering is important in connection with the energy spectrum[17] where it has a greater effect. The low-energy pions that arise from the inelastic scattering of very strongly interacting pions will be indistinguishable from the directly produced pions in nuclei which are large, that is $R \geq \lambda\!\!\!^{-}_{\text{total}}$. This condition is satisfied for most of the pions produced by the bremsstrahlung beam.

(5) The absorption mean free path is calculated by using a quasi-deuteron model[19] in which there is a parameter for the relative number of deuterons in the nucleus. The large size of this parameter required to fit other pion-nucleus interactions has been interpreted as indicating strong nucleon-nucleon correlations in nuclear matter.[27] The $(\pi^+ - d)$ interaction changes rapidly with pion energy, and multiple elastic scattering which is also strongly energy-dependent increases the path-length of the outgoing pion. One would expect to observe a somewhat shorter absorption mean free path than predicted on the quasi-deuteron model for the high-energy pions.

(6) Mean free paths obtained directly from pion scattering from nuclei[28] do not differ significantly from these results.

ACKNOWLEDGMENTS

We wish to thank all those who contributed to the design, construction, and operation of the pion-counting equipment, as well as those who provided the necessary high-energy bremsstrahlung: Dr. C. M. Newton, Dr. G. E. Masek, Dr. D. C. Hagerman, Dr. Hans Motz, and Mr. A. J. Lazarus were involved in the development of the equipment; Professor W. K. H. Panofsky, Professor R. F. Mozley, R. G. Gilbert, and the operators of the Mark III accelerator provided us with many hours of steady beam.

APPENDIX

The Z-dependent corrections will be calculated in three parts: (A) Pions are reflected at the surface, and the transmission coefficient due to the change in potential energy is calculated. (B) The real potential due to the pion-nucleon interaction and the nuclear Coulomb potential alters the kinetic energy of pions inside nuclear matter. The fundamental production cross section, being a steep function of pion energy, will thus vary with atomic number. (C) The imaginary potential causes pions to be attenuated as they cross the nucleus from the point of production to the surface.

(A) The usual Sommerfield factor for the Coulomb correction[29] is

$$C^+(0) = \frac{2\pi\eta}{\exp(+2\pi\eta)-1}, \tag{A1}$$

where η equals $Ze^2/\hbar v$. The Sommerfield factor must be evaluated at the nuclear surface rather than at the origin for the heavy elements. The barrier factor when the nuclear absorption is very strong is usually written as

$$v_L = (F_L{}^2 + G_L{}^2)^{-1}, \tag{A2}$$

where $F_L(\eta,\rho)$, $G_L(\eta,\rho)$ are the Coulomb wave functions,[30] where ρ equals kR, k equals $p/\hbar$, and R is the nuclear radius. Blatt and Weisskopf[31] give the transmission coefficient for charged particles for the other

---

[22] Evidence for approximately equal proton and neutron radii was reported by Abashian, Cool, and Cronin, Phys. Rev. **104**, 855 (1956).

[23] R. M. Friedman and K. M. Crowe, Phys. Rev. **105**, 1369 (1957).

[24] M. H. Johnson, Phys Rev. **83**, 510 (1951); K. W. McVoy, Jr., Cornell University doctoral dissertation (1956) (unpublished).

[25] Professor K. M. Watson has indicated the connection between the variation of the real potential and the inelastic pion scattering (private communication).

[26] Bernardini, Booth, and Lederman, Phys. Rev. **83**, 1075, 1277 (1951); Bernardini, Booth, Lederman, and Tinlot, Phys. Rev. **82**, 105 (1951).

[27] Brueckner, Eden, and Francis, Phys. Rev. **98**, 1445 (1955).

[28] F. H. Tenny and J. Tinlot, Phys. Rev. **92**, 974 (1953); A. M. Shapiro, Phys. Rev. **84**, 1063 (1951); Byfield, Kessler, and Lederman, Phys. Rev. **86**, 17 (1952); J. F. Tracy, Phys. Rev. **91**, 960 (1953); G. Bernardini and F. Levy, Phys. Rev. **84**, 610 (1951); D. Stork, Phys. Rev. **93**, 868 (1954).

[29] R. E. Marshak, *Meson Physics* (McGraw-Hill Book Company, Inc., New York, 1952), p. 97.

[30] Bloch, Hull, Broyles, Bouricius, Freeman, and Breit, Revs. Modern Phys. **23**, 147 (1951).

[31] J. M. Blatt and V. F. Weisskopf, *Theoretical Nuclear Physics* (John Wiley and Sons, Inc., New York, 1952), Chap. VIII.

extreme—when the absorption can be neglected:

$$t=\frac{4\epsilon v_L}{\epsilon^2+(2\epsilon+v_L')v_L};\tag{A3}$$

$$\epsilon=k_{\text{inside}}/k_{\text{outside}};\tag{A4}$$

$$v_L'=\frac{1}{k^2}\left[\frac{dG}{dr}+\frac{dF}{dr}\right]^2.\tag{A5}$$

For energies large compared with the Coulomb barrier, t approaches unity.

(B) The potential for pions in the nucleus is the sum of the real potential arising from the pion-nucleon interaction and the Coulomb energy. The Z-dependent effect due to the Coulomb energy can be estimated from the known behavior of the photomeson cross sections.[32] Considering s- and p-wave mesons only,

$$\sigma=A+B\cos\theta+C\cos^2\theta,\tag{A6}$$

where θ is the pion angle in the center-of-mass system. For a lab angle of 60°, the c.m. angle is near 90° so that for estimates we shall use the following expression for A:

$$A=\rho g_s+\rho p^2 g_p,\tag{A7}$$

where p is the c.m. pion momentum (in units μc) and

$$\rho=\frac{p}{\nu[1+(\nu\mu/M)][1+(p^2+1)^{\frac{1}{2}}(\mu/M)]},\tag{A8}$$

where ν is the photon momentum (in units μc), μ and M are the pion and nucleon masses, respectively. Therefore we have the approximate expression

$$\sigma\simeq C_s p+C_p p^3.\tag{A9}$$

In the production in a nucleus one must average over the pion momenta involved in the production.

Considering the s-state term only and replacing the average pion momentum by the momentum of the pion in the nuclear potential, we obtain an approximate expression:

$$\sigma_Z(\pi^+)\simeq Z\sigma_0\left[\frac{p(Z)_{\text{inside}}}{p_{\text{outside}}}\right]=Z\sigma_0\epsilon$$

$$\simeq Z\sigma_0\left(\frac{E-V-V_c}{E}\right)^{\frac{1}{2}},\tag{A10}$$

where E is the kinetic energy outside the nucleus, V is the real part of the optical potential of the pion in nuclear matter, and V_c is the Coulomb energy. For pion energies less than 60 Mev the real potential can be approximately expressed in terms of the kinetic energy K.E. as[19]

$$V=-0.40(\text{K.E.})=-0.40(E-V-V_c).\tag{A11}$$

The final factor becomes

$$\epsilon=\left\{\frac{5}{3}\left[\frac{(E-V_c)}{E}\right]\right\}^{\frac{1}{2}}.\tag{A12}$$

For high-energy pions, V must be found as a solution of the equation $V(\text{K.E.})=V(E-V-V_c)$ by using the potential variation given by Frank *et al.*[19] The p-state pions will be high enough in energy so that (A10) is not expected to be appropriate. We can base a crude estimate on (A9), however, which should be an upper limit to the Coulomb correction. The correction is small enough so that a more realistic estimate is not required.

(C) The absorption factor $f(x)$ is given by

$$f(x)=\frac{1}{\int_{\text{sphere}}d\tau}\int_{\text{sphere}}\exp(-D/\lambda_a)d\tau$$

$$=3\left[\frac{1}{2x}-\frac{1}{x^3}+\frac{1}{x^3}(e^{-x})(1+x)\right],\tag{A13}$$

and is the absorption average over the sphere of radius R; x equals $2R/\lambda_a$ where λ_a is the effective absorption mean free path; and D is the distance from the point of production to the surface.

When t is less than unity, the pion energies are small, and the absorption is not strong, and the approximations made for calculating t are good. The absorption factor has neglected the reflections from the boundaries so $f(x)$ will become less accurate for very low pion energies. In fact, as the pion energy drops below the Coulomb barrier energy, the pions arise from the surface layer corresponding to the tail of the smoothed or rounded-off charge distribution, a result which appears experimentally indistinguishable from an absorption mean free path of $\sim 1\times 10^{-13}$ cm for the heavy elements.

Combining the expressions for the transmission and absorption, we obtain (for s-wave mesons only),

$$\sigma\simeq Z\sigma_0\frac{4\epsilon^2 v_L}{\epsilon^2+(2\epsilon+v_L')v_L}f(x).\tag{A14}$$

By normalizing to one element (copper), σ_0 is eliminated. The expression (A14) should be appropriate for pions in the range under consideration.

[32] Watson, Keck, Tollestrup, and Walker, Phys. Rev. **101**, 1159 (1956). However, see M. J. Moravcsik, Phys. Rev. **104**, 1451 (1956), for a discussion of additional terms in Eq. (A6) for small angles.